The 9th European Congress on Computational Methods in Applied Sciences and Engineering
ECCOMAS Congress 2024
3–7 June 2024, Lisboa, Portugal

CONVERGENCE ANALYSIS OF MULTIRATE FIXED STRESS SPLIT WITH CONTACT MECHANICS

TAMEEM ALMANI[1], OSMAN HAMID[1], AND KUNDAN KUMAR[2]

[1] Saudi Aramco,
Dhahran, Saudi Arabia,
e-mails: tameem.almani@aramco.com, osman.hamid@aramco.com

[2] University of Bergen,
Bergen, Norway,
email: kundan.kumar@uib.no

Key words: Biot system, poroelasticity, fixed-stress split coupling, contact mechanics, contraction mapping

Summary. Several subsurface technologies involve injection of fluids at high pressure. An example is the extraction of the unconventional resources which involves well-stimulation techniques. One of the main well-stimulation techniques, especially for tight shale gas formations, is hydraulic fracturing. During this process, a fluid is injected into the formation at an extremely high pressure to initiate a network of fractures. The generated fractures are assumed to remain open, but this is not always the case. To accurately model the situation when fractures close back, one has to consider a coupled flow with geomechanics problem along with contact mechanics boundary conditions. Motivated by that, in this work, we extend the well-known single rate and multirate fixed-stress split coupling scheme to include frictionless contact mechanics boundary conditions for a poroelastic Biot model. In this model, a frictionless contact is assumed with the well-known Signorini condition in a form with a gap function. We state the results on the convergence of the extended single rate and multirate fixed-stress split schemes based on a fixed-point Banach contraction argument giving rise to the linear convergence of the corresponding scheme.

1 INTRODUCTION

Nowadays, as more tight gas and unconventional resources are being exploited worldwide, solving the coupled flow and geomechanics problem is becoming more important. This is due to the fact that to extract hydrocarbons trapped in these natural resources, well stimulation techniques, and in particular hydraulic fracturing, are often used to frack the formation to enhance recovery. Furthermore, once the hydraulic fracturing job is performed, proppants are injected into the natural and induced fractures to keep them open. Now, it is very clear that to model such a highly coupled problem, contact mechanics boundary conditions [1–5] should be incorporated into the underlying coupled model to accurately model fractures opening and closing, and also to determine the mechanical strength of the proppants needs to sustain the surrounding stress and keep the fractures open. Beyond hydraulic fracturing, the coupling of flow and mechanics in subsurface modeling has numerous applications. These include groundwater flow, geothermal

energy extraction, carbon sequestration, and underground hydrogen storage. In all these application areas, the interaction of flow, mechanics, and fractures or faults is critical to the risk management. The risk arises out of induced seismicity due to injection at high pressure or the leakage through the high permeable conduits facilitated by the fractures. The risk management requires an understanding of the mechanics of the fracture or the fault coupled to the flow and mechanical deformations in the porous matrix. In terms of simulation of these multiphysics processes, the challenge is in developing efficient numerical schemes for solving coupled flow and deformations in the presence of contact conditions.

Solving the coupled flow and mechanical deformations including the contact mechanics requires appropriate numerical approaches. For several reasons, the flow and mechanical problems are decoupled and solved in an iterative manner. These reasons include the use of existing separate legacy codes for flow and mechanics problems, development of efficient preconditioners based on block diagonal decoupling of the flow and mechanical effects, and flexibility with respect to time stepping for each of the two equations. The fixed stress split and the undrained split schemes are quite common iterative coupling scheme to solve the mechanical and flow problems that decouples these two effects. The two equations are solved in a sequential manner during every iterative coupling iteration, and a regularization term is added to the flow problem to stabilize the scheme and ensure convergence [6–8].

In this work, we announce the results concerning the convergence of the multirate schemes for the coupled flow and mechanics problems in presence of frictionless contact conditions. This extends the recent work presented in [9] to the multirate case. Here, the flow and mechanics problems assume two different time scales: a fine time scale for the flow problem, and a coarse time scale for the mechanics problem [10]. These methods exploit the difference in characteristic time scales for different physical effects. For example, we consider the mechanics to be quasi-static and the flow to be time dependent and in such a case, the time scale for mechanical effects is typically slower than the flow time scale. The computational efficiency considerations suggest solving mechanics on a coarse time scale and the flow being solved on a finer scale. Multirate schemes are accordingly designed to take several flow steps for each mechanics time step. This is an idea borrowed from the ODE literature, see for example [11] for solving a system of ODEs. In the current setting, we need to combine the multirate approaches with the iterative scheme that decouples flow and mechanics. Once the equations are decoupled, the multirate strategy involves solving several flow steps for each mechanics step. Accordingly, we consider a multirate extension of the fixed stress split iterative method for the Biot equations now also involving the (simplified) contact mechanics. For the case of the Biot model, multirate extensions of the undrained split and the fixed stress split schemes were proposed and analysed in [12–15]. In the previous work [9], the convergence of the single rate fixed stress split scheme was established with frictionless contact mechanics boundary conditions. Incorporating the contact mechanics boundary conditions led to a coupled system in which the mechanics equation is modeled through a variational inequality of the first kind [1, 9].

As stated above, in this work, we state the convergence of the multirate fixed stress split scheme with frictionless contact mechanics boundary conditions for the linear Biot model. It should be noted here the convergence of the standard fixed-stress split scheme was established in [7, 16, 17]

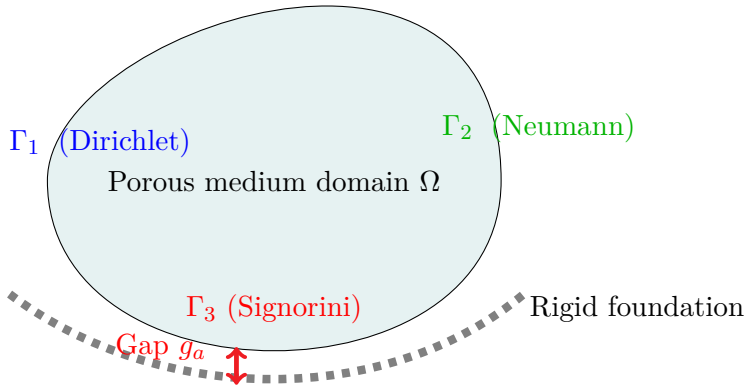

Figure 2.1: Frictionless contact of a porous medium with a rigid foundation with a gap function g_a

for the linear Biot model without fractures, and extended to fractured poro-elastic media in [18]. However, it was only in the recent work of [9] that contact mechanics boundary conditions were incorporated. In this paper, we announce the result that convergence still holds even when two different time scales are used: a coarse one for the mechanics problem, and a fine one for the flow problem.

The paper is organized as follows: Section (2) describes the Biot linear elastic model with frictionless contact mechanics boundary conditions. The mixed variational formulation is presented in Section (3). Section (4) presents our main result in this work for the multirate fixed stress split scheme, followed by Conclusions in Section (5).

2 BIOT LINEAR ELASTIC MODEL WITH FRICTIONLESS CONTACT MECHANICS BOUNDARY CONDITIONS

We adopt the same model as described in [1,9]. Let $\Omega \subset \mathbb{R}^d$ be a bounded domain ($d = 2, 3$). The boundary Γ is assumed to be smooth and split into three pairwise disjoint sets Γ_1, Γ_2, and Γ_3 such that $\Gamma = \bar{\Gamma}_1 \cup \bar{\Gamma}_2 \cup \Gamma_3$ as shown in Figure 2.1, with meas(Γ_1) > 0. We note here that Γ_1 represents the part of the boundary with Dirichlet mechanics boundary condition, Γ_2 for the Neumann traction boundary condition, and Γ_3 is the part of the boundary with the frictionless Signorini contact mechanics boundary condition.

2.1 Mechanics Model

The mechanics model with frictionless contact denoted by the Signorini condition in a form with a gap function in a porous medium is given as follows [1, 9]:

$$\nabla \cdot \boldsymbol{\sigma}^{\text{por}} + \boldsymbol{f}_0 = 0, \tag{2.1}$$

$$\boldsymbol{\sigma}^{\text{por}}(\boldsymbol{u}, p) = \boldsymbol{\sigma}(\boldsymbol{u}) - \alpha p \boldsymbol{I}, \tag{2.2}$$

$$\boldsymbol{\sigma}(\boldsymbol{u}) = \lambda(\nabla \cdot \boldsymbol{u})I + 2G\boldsymbol{\varepsilon}(\boldsymbol{u}), \tag{2.3}$$

$$\boldsymbol{\varepsilon}(\boldsymbol{u}) = \frac{1}{2}\left(\nabla \boldsymbol{u} + \nabla \boldsymbol{u}^T\right). \tag{2.4}$$

With the boundary conditions:

$$\boldsymbol{u} = 0 \quad \text{on} \quad \Gamma_1, \quad \boldsymbol{\sigma\nu} = \boldsymbol{f}_2 \quad \text{on} \quad \Gamma_2, \tag{2.5}$$

$$u_\nu \leq g_a, \ \sigma_\nu \leq 0, \ \sigma_\nu(u_\nu - g_a) = 0 \quad \text{on} \quad \Gamma_3, \tag{2.6}$$

$$\boldsymbol{\sigma}_\tau = 0 \quad \text{on} \quad \Gamma_3. \tag{2.7}$$

in which $\boldsymbol{u}$ is the displacement field ($\boldsymbol{u} : \Omega \mapsto \mathbb{R}^d$) and σ is the stress field ($\sigma : \Omega \mapsto \mathbb{S}^d$), where $\mathbb{S}^d$ is the space of second order symmetric tensors on $\mathbb{R}^d$. In the above, (2.1) is the balance of linear momentum equation (in quasi-static form, ignoring the second order time derivatives of displacements), (2.2) is the effective stress equation (subtracting the pore pressure contribution from the stress field), (2.3) is the standard definition of the stress field (Hooke's law) under homogeneous media and isotropic assumptions, and finally (2.4) is the linear strain equation. Furthermore, the gap between the domain and foundation is denoted by ($g_a > 0$) (a strictly positive given scalar). The Signorini contact mechanics boundary conditions are given by equation (2.6) with the gap function g_a. The first condition in (2.6) ensures that the normal component of the displacement is less than the initial gap g_a, the second condition ensures that the normal stress is always compressive, and the third condition is a complementarity condition ensuring that the normal stress vanishes when the normal displacement is less than the initial gap g_a. The boundary condition given by (2.7) ensures the frictionless case (the tangential component of the stress equals zero). Finally, the homogeneous Dirichlet boundary condition on Γ_1 and the traction Neumann boundary condition on Γ_2 are specified by (2.5). We note here that $u_\nu = \boldsymbol{u} \cdot \boldsymbol{\nu}, \sigma_\nu = (\boldsymbol{\sigma\nu}) \cdot \boldsymbol{\nu}$, $\boldsymbol{\sigma}_\tau = \boldsymbol{\sigma\nu} - \sigma_\nu \boldsymbol{\nu}$. We refer the reader to [1, 9] for more details on the model considered above.

2.2 Flow Model

In this work, we consider a slightly compressible singe phase flow model. The conservation of mass is given by: The flow equation consists of the mass balance equation:

$$\frac{\partial}{\partial t}\Big((\frac{1}{M} + c_f\varphi_0)p + \alpha\nabla \cdot \boldsymbol{u}\Big) + \nabla \cdot \boldsymbol{z} = q. \tag{2.8}$$

We note here that $\boldsymbol{z}$ is the flux variable, which is given by the Darcy law as follows: The flux $\boldsymbol{z}$ is described by the Darcy law.

$$\boldsymbol{z} = -\frac{1}{\mu_f}\boldsymbol{K}(\nabla\, p - \rho_{f,r} g \nabla\, \eta). \tag{2.9}$$

In the above, p is the pore pressure, $1/M$ is the solid matrix compressibility coefficient, c_f is the fluid compressibility, ϕ_0 is the initial porosity, μ_f is the fluid viscosity, $\rho_{f,r}$ is the fluid reference (constant) density, and α is the Biot coefficient.

3 MIXED VARIATIONAL FORMULATION

A mixed finite element formulation will be used for the flow and a conformal Galerkin formulation will be used for the contact mechanics problem. For time discretization, the standard backward-Euler scheme will be used. Using the lowest order Raviart-Thomas (RT) spaces, and assuming a family of conforming triangular elements covering the domain of interest $\overline{\Omega}$, and denoted by $\mathfrak{T}_h$, our discrete spaces are given as follows (Q_h for discrete pressures, V_h for discrete displacements, and Z_h for discrete fluxes):

$$V_h = \{\boldsymbol{v}_h \in H^1(\Omega)^d \,;\, \forall T \in \mathfrak{T}_h, \boldsymbol{v}_{h|T} \in {\mathbb{P}_1}^d, \boldsymbol{v}_{h|\Gamma_1} = \boldsymbol{0}\} \tag{3.10}$$

$$Q_h = \{p_h \in L^2(\Omega) \,;\, \forall T \in \mathfrak{T}_h, p_{h|T} \in \mathbb{P}_0, p_h = 0 \,\text{on}\, \Gamma\} \tag{3.11}$$

$$Z_h = \{\boldsymbol{q}_h \in H(\mathrm{div};\Omega)^d \,;\forall T \in \mathfrak{T}_h, \boldsymbol{q}_{h|T} \in {\mathbb{P}_1}^d,\, \boldsymbol{q}_h \cdot \nu = 0 \;\text{ on } \Gamma\} \tag{3.12}$$

In what follows, we first derive a variational inequality for the contact mechanics problem, then we will be ready to write our weak formulation of the coupled contact mechanics problem.

3.1 Variational Inequality of The First Kind

In continuous settings, we define the space of displacements as follow:

$$V_u := \left\{\boldsymbol{v} \in H^1(\Omega)^d : \boldsymbol{v} = 0 \text{ a. e. on } \Gamma_1, \boldsymbol{v}_\nu \leq g_a\right\}$$

Now, following the standard procedure, we multiply (2.1) by a test function $\boldsymbol{v} \in V_u$, and integrate by parts to derive the following weak formulation [1, 9]:

Finds $\boldsymbol{u} \in V_u$ such that

$$\begin{aligned} 2G\left(\boldsymbol{\varepsilon}(\boldsymbol{u}), \boldsymbol{\varepsilon}(\boldsymbol{v}) - \boldsymbol{\varepsilon}(\boldsymbol{u})\right)_\Omega + \lambda\left(\nabla \cdot \boldsymbol{u}, \nabla \cdot \boldsymbol{v} - \nabla \cdot \boldsymbol{u}\right) - \alpha\left(p, \nabla \cdot \boldsymbol{v} - \nabla \cdot \boldsymbol{u}\right) \\ = (\sigma_\nu, v_\nu - u_\nu)_{\Gamma_3} + (\boldsymbol{f}_0, \boldsymbol{v} - \boldsymbol{u}) + (\boldsymbol{f}_2, \boldsymbol{v} - \boldsymbol{u})_{\Gamma_2} + (\sigma_\tau, v_\tau - u_\tau)_{\Gamma_3} \end{aligned} \tag{3.13}$$

for all $\boldsymbol{v} \in V_u$. We note here that the last term in (3.13) vanishes as $\sigma_\tau = 0$ on Γ_3. In addition, the term $(\sigma_\nu, v_\nu - u_\nu)_{\Gamma_3}$ can be expanded as: $(\sigma_\nu, v_\nu - u_\nu)_{\Gamma_3} = (\sigma_\nu, (v_\nu - g_a) - (u_\nu - g_a))_{\Gamma_3} = (\sigma_\nu, (v_\nu - g_a))_{\Gamma_3}$ using the condition $\sigma_\nu(u_\nu - g_a) = 0$. Furthermore, using the two conditions: $u_\nu - g_a \leq 0$ (recall that $\boldsymbol{u} \in V_u$) and $\sigma_\nu \leq 0$, the weak formulation now reads:

Find $\boldsymbol{u} \in V_u$ such that

$$\begin{aligned} 2G\left(\boldsymbol{\varepsilon}(\boldsymbol{u}), \boldsymbol{\varepsilon}(\boldsymbol{v}) - \boldsymbol{\varepsilon}(\boldsymbol{u})\right)_\Omega + \lambda\left(\nabla \cdot \boldsymbol{u}, \nabla \cdot \boldsymbol{v} - \nabla \cdot \boldsymbol{u}\right) - \alpha\left(p, \nabla \cdot \boldsymbol{v} - \nabla \cdot \boldsymbol{u}\right) \\ \geq (\boldsymbol{f}_0, \boldsymbol{v} - \boldsymbol{u}) + (\boldsymbol{f}_2, \boldsymbol{v} - \boldsymbol{u})_{\Gamma_2} \end{aligned}$$

for all $\boldsymbol{v} \in V_u$.

Next, assume that the pressure p is given. Define:

$$\begin{aligned} (\boldsymbol{u}, \boldsymbol{v})_Q &:= 2G\left(\boldsymbol{\varepsilon}(\boldsymbol{u}), \boldsymbol{\varepsilon}(\boldsymbol{v})\right)_\Omega + \lambda\left(\nabla \cdot \boldsymbol{u}, \nabla \cdot \boldsymbol{v}\right) - \alpha\left(p, \nabla \cdot \boldsymbol{v}\right) \\ (\boldsymbol{f}, \boldsymbol{v})_V &:= (\boldsymbol{f}_0, \boldsymbol{v} - \boldsymbol{u})_\Omega + (\boldsymbol{f}_2, \boldsymbol{v} - \boldsymbol{u})_{\Gamma_2} \end{aligned}$$

for all $\boldsymbol{v} \in V_u$.

Therefore, we retrieve the variational inequality of the first kind:

Find $\boldsymbol{u} \in V_u$ such that

$$(\boldsymbol{u}, \boldsymbol{v} - \boldsymbol{u})_Q \geq (\boldsymbol{f}, \boldsymbol{v} - \boldsymbol{u})_V$$

for all $\boldsymbol{v} \in V_u$.

3.2 Weak Formulation

We write down the weak formulation in the discrete form:

(**Flow equation in discrete form**) Find $p_h^k \in Q_h$ and $\boldsymbol{z}_h^k \in Z_h$ such that

$$\begin{aligned} \forall \theta_h \in Q_h \,, \frac{1}{\Delta t}\Big((\frac{1}{M} + c_f \varphi_0)\Big(p_h^k - p_h^{k-1}\Big), \theta_h\Big) + \frac{1}{\mu_f}(\nabla \cdot \boldsymbol{z}_h^k, \theta_h) = \\ - \frac{\alpha}{\Delta t}\Big(\nabla \cdot \Big(\boldsymbol{u}_h^k - \boldsymbol{u}_h^{k-1}\Big), \theta_h\Big) + \Big(q_h, \theta_h\Big), \end{aligned} \tag{3.14}$$

$$\forall \boldsymbol{q}_h \in Z_h \,, \Big(\boldsymbol{K}^{-1} \boldsymbol{z}_h^k, \boldsymbol{q}_h\Big) = \Big(p_h^k, \nabla \cdot \boldsymbol{q}_h\Big) + \Big(\rho_{f,r} g \nabla \eta, \boldsymbol{q}_h\Big), \tag{3.15}$$

(**Mechanics equation in discrete form**) Find $\boldsymbol{u}_h^k \in V_h$ such that for all $\boldsymbol{v}_h \in V_h$

$$(\boldsymbol{u}_h^k, \boldsymbol{v}_h - \boldsymbol{u}_h^k)_Q \geq (\boldsymbol{f}, \boldsymbol{v}_h - \boldsymbol{u}_h^k)_V, \tag{3.16}$$

with the following initial conditions for the first time step: $p_h^0 = p_0$ and $\boldsymbol{u}_h^0 = \boldsymbol{u}_0$. To ensure the well-posedness of the model equations, we assume the compatibility of the initial data [19].

4 MULTIRATE FIXED STRESS SPLIT FOR FRICTIONLESS CONTACT PROBLEM

To contrast the multirate scheme with the traditional single rate scheme (same time step for flow as well as for mechanics equations), we start with the single rate fixed stress split scheme for the frictionless contact problem. Table 4.1 summarizes the major differences between these two schemes when solving the coupled flow and mechanics problem.

Remark 4.1 (Remark on Notation)**.** *In what follows, we assume the following notation: n denotes the iterative coupling iteration index, k is the time step index in the single rate scheme and the coarse mechanics time step index in the multirate scheme (k is a multiple of q in the multirate scheme, and q is the number of flow fine time steps within one coarse mechanics time step), and m is the local fine flow time step index in the multirate scheme ($1 \leq m \leq q$). We note here that as n approaches infinity, the scheme converges to the fully implicit scheme.*

4.1 SINGLE RATE FIXED STRESS SPLIT

As stated in [9], the numerical scheme for the single rate fixed stress split algorithm for the frictionless contact problem splits the problem in flow solve followed by the mechanics solve.

Table 4.1: Single Rate versus Multirate Flow-Mechanics Coupling

Feature	Single-Rate Coupling Scheme	Multirate Coupling Scheme
Time-Stepping	Single time step for both flow and mechanics	fine time steps for flow, coarse for mechanics
Computational Cost	Higher due to frequent mechanics couplings	Lower due to less frequent mechanics couplings
Accuracy	More accurate coupling between flow and mechanics	May introduce errors if time steps are not selected carefully
Implementation Complexity	Straightforward	More complex due to different time scales
Flexibility	Limited flexibility in adapting physical time scales	Flexible physics-driven time-stepping for flow and mechanics

The flow problem is stabilised by adding a term on the diagonal of the pressure matrix. The scheme is given as follows:

Step (a): Flow step: Find $p_h^{n+1,k} \in Q_h$, $\boldsymbol{z}_h^{n+1,k} \in Z_h$ such that:

$$\forall \theta_h \in Q_h\,,\ \Big((\frac{1}{M} + c_f\varphi_0 + \frac{\alpha^2}{\lambda})(\frac{p_h^{n+1,k} - p_h^{k-1}}{\Delta t}), \theta_h\Big) + \frac{1}{\mu_f}(\nabla \cdot \boldsymbol{z}_h^{n+1,k}, \theta_h) =$$
$$\Big(- \frac{\alpha}{\lambda}(- \alpha(\frac{p_h^{n+1,k} - p_h^{k-1}}{\Delta t}) + \lambda \nabla \cdot (\frac{\boldsymbol{u}_h^{n+1,k} - \boldsymbol{u}_h^{k-1}}{\Delta t})), \theta_h\Big) + (q_h, \theta_h), \tag{4.17}$$

$$\forall \boldsymbol{q}_h \in Z_h\,,\ (\boldsymbol{K}^{-1}\boldsymbol{z}_h^{n+1,k}, \boldsymbol{q}_h) = (p_h^{n+1,k}, \nabla \cdot \boldsymbol{q}_h) + (\nabla(\rho_{f,r} g\eta), \boldsymbol{q}_h). \tag{4.18}$$

Step (b): Mechanics step: With $p_h^{n+1,k} \in Q_h$ computed from the flow step, find $\boldsymbol{u}_h^{n+1,k} \in V_h$ such that for all $v_h \in V_h$

$$(\boldsymbol{u}_h^{n+1,k}, \boldsymbol{v}_h - \boldsymbol{u}_h^{n+1,k})_Q \geq (\boldsymbol{f}, \boldsymbol{v}_h - \boldsymbol{u}_h^{n+1,k})_V. \tag{4.19}$$

We comment on the structure of the above scheme. The first equation describing the evolution of the pressure is stabilized with $(\alpha^2/\lambda)p_h^{n+1,k}$ term being added on the left hand side. Moreover, to ensure consistency a similar term with pressure term being iteration lagged is added to the right hand side. The convergence of the above scheme yields the solution of above discrete weak form (3.14) - (3.16). In what follows, the convergence theorems will be shown in terms of differences between coupling iterates within every time step. For a particular time step $t = t_k$, we will denote the difference as follows:

$$\delta\xi^{n+1,k} = \xi^{n+1,k} - \xi^{n,k},$$

where ξ can represent $p_h, \boldsymbol{z}_h$, or $\boldsymbol{u}_h$. As derived in [9], the scheme above converges to the unique solution of the coupled problem thanks to the following theorem:

Theorem 1. *Define* $\sigma_v^{n,k}$ *as* $\sigma_v^{n,k} := \lambda\nabla\cdot\boldsymbol{u}_h^{n,k} - \alpha(p_h^{n,k} - p_h^{k-1})$. *The iterative scheme defined by* (4.17) - (4.19) *is a contraction given by*

$$\begin{aligned}&\left\|\delta\sigma_v^{n+1,k}\right\|_\Omega^2 + \tfrac{2\Delta t\lambda M\alpha^2}{\mu_f(M\alpha^2+\lambda(1+Mc_f\varphi_0))}\left\|\boldsymbol{K}^{-1/2}\delta\boldsymbol{z}_h^{n+1,k}\right\|_\Omega^2 + 4G\lambda\|\varepsilon(\delta\boldsymbol{u}_h^{n+1,k})\|_\Omega^2\\ &+\lambda^2\|\nabla\cdot\delta\boldsymbol{u}_h^{n+1,k}\|_\Omega^2 \leq \left(\tfrac{M\alpha^2}{\lambda+M\lambda c_f\varphi_0+M\alpha^2}\right)^2\left\|\delta\sigma_v^{n,k}\right\|_\Omega^2.\end{aligned}$$

In the above theorem, we notice that $\left(\frac{M\alpha^2}{\lambda+M\lambda c_f\varphi_0+M\alpha^2}\right)^2 < 1$ implying that this is contraction. We also notice that when M (compressibility is small) is large, the convergence is slower. In the above theorem, the contraction is achieved for $\sigma_v^{n,k}$ which is a composite quantity of $\nabla\cdot\boldsymbol{u}_h^{n,k}$ and $p_h^{n,k}$. The convergence to the physical variables is achieved by the convergence of $\sigma_v^{n,k}$ together with the remaining terms on the left hand side in the above theorem. This ensures the convergence of this scheme to the unique solution of the coupled weak form (3.14) - (3.16). An alternative approach is to get the contraction estimate directly in terms of physical variables in their natural energy norms as followed in [20, 21]. The choice of stabilization factor determines the contraction factor. We expect that the smaller this contraction coefficient, the number of iterations needed to achieve a desired tolerance will be smaller. However, this turns out to be more delicate. In fact, this is dependent on the full H^2 estimate from the control of $-\Delta$ in a domain. As shown in [22], the optimal number of iterations depends on the domain and the boundary conditions.

The extension to the multirate scheme, in which the flow takes multiple fine time step within one coarse mechanics time step requires choosing the appropriate iteration between flow and mechanics equation. The multirate weak formulation of the coupled contact model reads [10]:

For $k = iq$, $i \in \mathbb{N}$, $n = 1, 2, ..$

- **Step (a):** q **Fine Flow Steps:** For $1 \leq m \leq q$, find $p_h^{n+1,m+k} \in Q_h$, and $\boldsymbol{z}_h^{n+1,m+k} \in Z_h$ such that,

$$\begin{aligned}&\forall\theta_h \in Q_h\,,\ \frac{1}{\Delta t}\Big((\frac{1}{M}+c_f\varphi_0+L)\Big(p_h^{n+1,m+k}-p_h^{n+1,m-1+k}\Big),\theta_h\Big)\\ &\quad+\frac{1}{\mu_f}(\nabla\cdot\boldsymbol{z}_h^{n+1,m+k},\theta_h) = \frac{1}{\Delta t}\Big(L\Big(p_h^{n,m+k}-p_h^{n,m-1+k}\Big)\\ &\qquad-\frac{\alpha}{q}\nabla\cdot\Big(\boldsymbol{u}_h^{n,k+q}-\boldsymbol{u}_h^{n,k}\Big),\theta_h\Big)+\Big(\tilde{q}_h,\theta_h\Big),\end{aligned}\tag{4.20}$$

$$\forall\boldsymbol{q}_h \in \boldsymbol{Z}_h\,,\ \Big(\boldsymbol{K}^{-1}\boldsymbol{z}_h^{n+1,m+k},\boldsymbol{q}_h\Big) = \Big(p_h^{n+1,m+k},\nabla\cdot\boldsymbol{q}_h\Big)+\Big(\rho_{f,r}g\nabla\,\eta,\boldsymbol{q}_h\Big).\tag{4.21}$$

- **Step (b): Coarse Mechanics Step:** Given $p_h^{n+1,k+q}$ and $\boldsymbol{z}_h^{n+1,k+q}$, find $\boldsymbol{u}_h^{n+1,k+q} \in V_h$ such that,

$$(\boldsymbol{u}_h^{n+1,k+q},\boldsymbol{v}_h-\boldsymbol{u}_h^{n+1,k+q})_Q \geq (\boldsymbol{f},\boldsymbol{v}_h-\boldsymbol{u}_h^{n+1,k+q})_V.\tag{4.22}$$

We note the mathematical structure of the above scheme. The pressure equations and the displacement equations are decoupled. The displacement equation is in fact a variational inequality

due to the contact mechanics terms. The variational inequality arises from the Signorini condition. Moreover, we need to solve q elliptic equations (arising out of time discretization of parabolic pressure equation) followed by a mechanics solve which uses the pressure solution after q flow solves in the first step. The flexibility of choosing several time steps for one mechanics time step can be used to design parallel in time algorithm [23]. Below, we state our main contraction result in this work:

Theorem 2. *For $1 \leq m \leq q$, define $\sigma_v^{n,m+k}$ as $\sigma_v^{n,m+k} = (p_h^{n,m+k} - p_h^{n,m-1+k}) - \frac{\alpha}{qL}\nabla \cdot \boldsymbol{u}_h$. For $L = \frac{\alpha^2}{\lambda}$, $c_0 = \frac{2Lq}{\chi^2}$, and $\beta = \frac{1}{M} + c_f\varphi_0 + L$, the multirate iterative scheme is a contraction given by*

$$
\begin{aligned}
&2Gc_0\|\boldsymbol{\varepsilon}(\delta \boldsymbol{u}_h^{n+1,k+q})\|^2 + \textstyle\sum_{m=1}^{q} \left\|\delta\sigma_v^{n+1,m+k}\right\|^2 + \frac{\Delta t}{\beta\mu_f}\left\|\boldsymbol{K}^{-1/2}\delta \boldsymbol{z}_h^{n+1,k+q}\right\|^2 \\
&+\frac{\Delta t}{\beta\mu_f}\textstyle\sum_{m=1}^{q}\left\|\boldsymbol{K}^{-1/2}(\delta \boldsymbol{z}_h^{n+1,m+k} - \delta \boldsymbol{z}_h^{n+1,m-1+k})\right\|^2 \\
&\qquad\qquad \leq \left(\frac{M\alpha^2}{\lambda + M\lambda c_f\varphi_0 + \alpha^2 M}\right)^2 \textstyle\sum_{m=1}^{q}\left\|\delta\sigma_v^{n,m+k}\right\|^2.
\end{aligned}
$$

We mention some remarks and contrast this result to the single rate result in Theorem 1. First, in the above scheme, we have kept the stabilisation factor L as an unknown to be determined by the proof. The theorem provides the value of L that ensures convergence and the same value of L is also sufficient to provide the convergence in the single rate case. Interestingly, the convergence rate is determined by the same contraction factor as in the single rate case, namely $\left(\frac{M\alpha^2}{\lambda + M\lambda c_f\varphi_0 + \alpha^2 M}\right)^2 < 1$. The question of accuracy however is not addressed in this theorem. In general, we expect the error to be less than the single rate case with $q\Delta t$ time step. But the theoretical error estimates only provide rather pessimistic error estimates of the order $q\Delta t$. Another question is how to choose q. We note that a smaller q leads to higher computational cost whereas the lower q saves computational costs as fewer mechanical steps are needed. However, this may be more delicate in more complex situations including nonlinear mechanics and multiphase flow models where the larger time step of mechanics may lead to slow convergence requiring more iterative steps. The appropriate value of q therefore has to be decided by a posteriori error estimates. This remains to be addressed in a future work.

The proof of the above contraction theorem consists of 3 steps. In the first step, we estimate the flow problem getting the energy estimates. The estimates for the flow provides the L^2 norm of the pressure and that of the fluxes. These estimates involve the coupling terms of pressure and displacement which needs to be resolved using the help from the mechanics step. Next, we estimate the mechanics step using the variational inequality. This yields the H^1 norm estimate for the displacement, however there is a coupling term containing pressure and displacement that remains to be estimated. In the third step, we combine the flow and mechanics step and use the composite quantities $\sigma_v^{n,m+k}$ to get estimates. The coupling terms are subsumed in this composite quantity. Some algebraic manipulations then complete the proof of contraction. This however keeps the question of convergence of the physical variables still open. We note that we have a variational inequality, pressure at fine time steps, and displacement at coarse time steps. The convergence of these terms requires again the remaining terms on the left hand side of the above theorem, mathematical induction, and nonlinear PDE arguments to complete the steps. We omit the details of the proof in this paper, as it will be addressed elsewhere.

5 CONCLUSIONS

In this work, we extend single rate and multirate fixed-stress split schemes to include frictionless contact mechanics boundary conditions. The well-known Signorini condition [1] is used to model the frictionless contact in a form with a gap function in a porous medium. The convergence of the single rate fixed-stress split scheme with the Signorini condition was rigorously derived in [9]. In this paper, we state an analogous result for the multirate fixed-stress split scheme with the same condition (the Signorini condition). The detailed convergence proof will presented in a detailed manuscript outside the scope of this short paper. It should be noted here that the convergence analysis can be extended to other flow-mechanics coupling schemes, including the undrained split scheme, which we will consider next. Furthermore, numerical simulations will be considered in a future work to include the friction case as well.

REFERENCES

[1] M. Sofonea and A. Matei. *Mathematical models in contact mechanics*. Number 398. Cambridge University Press, 2012.

[2] M. V. de Hoop and K. Kumar. Coupling of flow, contact mechanics and friction, generating waves in a fractured porous medium. *arXiv preprint arXiv:2308.04338*, 2023.

[3] L. Banz and F. Bertrand. Contact problems in porous media. *arXiv preprint arXiv:2302.02600*, 2023.

[4] A. Hosseinkhan and R. E. Showalter. Biot-pressure system with unilateral displacement constraints. *Journal of Mathematical Analysis and Applications*, 497(1):124882, 2021.

[5] A. Hosseinkhan and R. E. Showalter. Semilinear degenerate biot–signorini system. *SIAM Journal on Mathematical Analysis*, 55(5):5643–5665, 2023.

[6] A. Settari and F.M. Mourits. A coupled reservoir and geomechanical simulation system. *SPE J.*, 3(3):219–226, 1998.

[7] J. Kim, H. A. Tchelepi, and R. Juanes. Stability, accuracy, and efficiency of sequential methods for coupled flow and geomechanics. *The SPE Reservoir Simulation Symposium, Houston, Texas, 2009.*, (SPE119084), 2009.

[8] V. Girault, K. Kumar, and M. F. Wheeler. Convergence of iterative coupling of geomechanics with flow in a fractured poroelastic medium. *Comput. Geosci.*, 20(5):997–1011, 2016.

[9] T. Almani and K. Kumar. Fixed stress splitting approach for contact problems in a porous medium. *arXiv preprint arXiv:2407.13459*, 2024.

[10] T. Almani, K. Kumar, A. Dogru, G. Singh, and M.F. Wheeler. Convergence analysis of multirate fixed-stress split iterative schemes for coupling flow with geomechanics. *Computer Methods in Applied Mechanics and Engineering*, 311:180 – 207, 2016.

[11] V. Savcenco, W. Hundsdorfer, and J. G. Verwer. A multirate time stepping strategy for stiff ordinary differential equations. *BIT Numerical Mathematics*, 47(1):137–155, 2007.

[12] T. Almani, K. Kumar, A. Dogru, G. Singh, and M.F. Wheeler. Convergence analysis of multirate fixed-stress split iterative schemes for coupling flow with geomechanics. *Computer Methods in Applied Mechanics and Engineering*, 311:180 – 207, 2016.

[13] K. Kumar, T. Almani, G. Singh, and M. F. Wheeler. *Multirate Undrained Splitting for Coupled Flow and Geomechanics in Porous Media*, pages 431–440. Springer International Publishing, Cham, 2016.

[14] T. Almani, S. Lee, T. Wick, and M. F. Wheeler. Multirate coupling for flow and geomechanics applied to hydraulic fracturing using an adaptive phase-field technique. In *The SPE Reservoir Simulation Conference*, 2017. SPE-182610-MS.

[15] R. Ye, K. Kumar, M. V. de Hoop, and M. Campillo. A multi-rate iterative coupling scheme for simulating dynamic ruptures and seismic waves generation in the prestressed earth. *Journal of Computational Physics*, 405:109098, 2020.

[16] A. Mikelić and M. F. Wheeler. Theory of the dynamic Biot-Allard equations and their link to the quasi-static Biot system. *J. Math. Phys.*, 53(12):123702, 15, 2012.

[17] T. Almani, K. Kumar, and M. F. Wheeler. Convergence and error analysis of fully discrete iterative coupling schemes for coupling flow with geomechanics. *Comput. Geosci.*, 21(5-6):1157–1172, 2017.

[18] V. Girault, K. Kumar, and M. F. Wheeler. Convergence of iterative coupling of geomechanics with flow in a fractured poroelastic medium. *Computational Geosciences*, 20(5):997–101, 2016.

[19] R. E. Showalter. Diffusion in poro-elastic media. *J. Math. Anal. Appl.*, 251(1):310–340, 2000.

[20] J. W. Both, M. Borregales, J. M. Nordbotten, K. Kumar, and F. A. Radu. Robust fixed stress splitting for the biot equations in heterogeneous media. *Applied Mathematics Letters*, 68:101–108, 2017.

[21] M. Borregales, F. A. Radu, K. Kumar, and J. M. Nordbotten. Robust iterative schemes for non-linear poromechanics. *Computational Geosciences*, 22:1021–1038, 2018.

[22] E. Storvik, J. W. Both, K. Kumar, J. M. Nordbotten, and F. A. Radu. On the optimization of the fixed-stress splitting for the biot equations. *International Journal for Numerical Methods in Engineering*, 120(2):179–194, 2019.

[23] M. Borregales, K. Kumar, F. A. Radu, C. Rodrigo, and F. J. Gaspar. A partially parallel-in-time fixed-stress splitting method for biot's consolidation model. *Computers & Mathematics with Applications*, 77(6):1466–1478, 2019.